PHYSICAL REVIEW A **73**, 021402(R) (2006)

Controlling vibrational wave packets with intense, few-cycle laser pulses

Hiromichi Niikura,[1,2,*] D. M. Villeneuve,[1] and P. B. Corkum[1]
[1]*National Research Council of Canada, 100 Sussex Drive, Ottawa, Ontario, Canada K1A 0R6*
[2]*PRESTO, Japan Science and Technology Agency, 4-1-8 Honcho Kawaguchi, Saitama, Japan*
(Received 11 April 2005; published 7 February 2006)

Using three precisely timed laser pulses, we show experimentally that subvibrational period, nonresonant laser radiation can control a vibrational wave packet. One pulse launches the wave packet and the second modifies the potential energy surfaces as the wave packet moves and the third probes its time evolution by Coulomb explosion imaging. First, we observe D_2^+ wave packets up to the first half revival without a control pulse. Next, we apply the control pulse to split the wave packet when the wave packet is near the outer turning point. We observe that one piece remains in the bound state and the other propagates to the dissociation continuum. By varying the delay between the pump and control pulses, we control the branching ratios. By a quantum mechanical calculation, we also show that if carrier-envelope phases of subvibrational period pulses are controlled, it can break left-right symmetry during dissociation, freezing the electron on one of the two dissociating fragments during dissociation.

DOI: 10.1103/PhysRevA.73.021402 PACS number(s): 42.50.Hz, 33.80.Rv

Controlling reaction dynamics is a major aim of photochemistry [1]. Recently, control of the final product yield has been achieved using adaptive shaping of intense, nonresonant ultrashort laser pulses [2]. However, since adaptive control relies on optimizing a laser pulse shape in order to maximize a certain product yield, the mechanisms of control are often obscure.

To identify some of the underlying mechanisms that allow control of molecular dynamics, we concentrate on the simplest molecule, D_2^+ and subvibrational period laser pulses. A short pulse allows us to create well-defined wave packets, and allows us to interact with them when they are localized. Our results rely on recent advances in laser technology that permit the generation of few-cycle, carrier-envelope phase-controlled laser pulses [3].

Using three independently delayed few-cycle pulses, we launch a wave packet, control its motion using the ac Stark shift, and probe its time evolution by Coulomb explosion. This is a major advance on a previous experiment in which an optical beat between two 50 fs ir pulses launches and controls a wave packet (with no probe) [4]. We apply a nonresonant intense laser field to modify the potential energy surface. Depending on the time at which the control pulse is applied, the wave packet can be directed towards dissociation, remain bound, or split into bound and dissociative components. Using Coulomb explosion imaging, we observe the time evolution of the D_2^+ wave packet.

The control mechanisms rely on using the laser-induced dipole force to modify the potential energy surfaces at the correct time. Laser-induced dipole forces are widely used to control atomic motion [5] where intensity and proximity to resonance are the control parameters. In molecules, isolated resonances are rarely available. Intensity, phase and pulse duration are the control parameters. They are already used to control alignment [6], orientation [7], and translational motion [8] of molecules.

*Email address: Hiromichi.Niikura@nrc.ca

Figure 1 plots the important potential energy surfaces of D_2^+ and D_2^{2+} together with the excitation processes. The pump pulse launches a vibrational wave packet on the $D_2^+(X\,\Sigma_g)$ surface by tunnel ionization [9]. A delayed control pulse, with polarization parallel to the molecular axis, separates the $D_2^+(X\,\Sigma_g)$ and $D_2^+(A\,\Sigma_u)$ surfaces by the field-induced Stark shift [4,10]. The dotted lines in Fig. 1 represent the field-modified potentials averaged over one optical period calculated for a laser intensity of 1.3×10^{14} W/cm^2. The probe pulse removes the remaining electron and projects the vibrational wave packet to the D_2^{2+} state, leading to D^+ fragments whose kinetic energy spectrum is a measure of the square of the vibrational wave packet on the D_2^+ surfaces. By changing the delay between the pump and the control pulses, we control the time evolution of the vibrational wave packet.

Our experiment is performed in a time-of-flight (TOF) mass spectrometer containing D_2 molecules [9]. The ions are extracted by a dc electric field applied between two electrodes separated by 3 cm and detected by a microchannel plate. We only detect fragments that pass through a 1 mm hole on one of the electrodes with a certain acceptance angle [9]. Thus, if the laser pulse is polarized parallel (perpendicular) to the TOF axis, it is also parallel (perpendicular) to the molecular axis of those molecules whose fragments are detected.

We focus an 800 nm, 40 fs, 400 μJ laser pulse produced by a Ti:sapphire laser of standard design into a hollow core fiber filled with argon gas. Self-phase modulation broadens the bandwidth of the input pulse in the range 650 nm–900 nm [11]. The output pulse from the fiber is compressed by six reflections on two pairs of the chirped mirrors. We further compensate the chirp by inserting thin quartz plates in the optical path before the vacuum chamber. To minimize the laser pulse duration, we adjust the thickness of the quartz plates so that the peak of the kinetic energy distribution is ~6.5 eV per fragment, corresponding to a pulse duration of ~8 fs [12]. The intensity background of

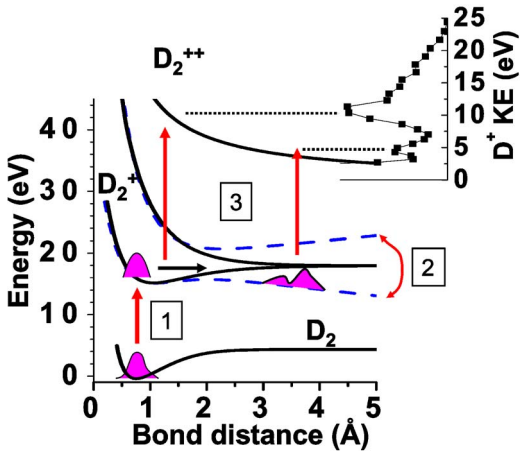

FIG. 1. (Color online) The selected potential energy surfaces of D_2^+ and D_2^{2+}. A pump pulse creates a vibrational wave packet on the $D_2^+(X\,\Sigma_g)$ surface. A delayed control pulse modifies the potential energy surfaces (dotted lines). The probe pulse further ionizes D_2^+ to D_2^{2+}, leading to D^+ fragments. Kinetic energy distribution of D^+ (inset) is a measure of the bond distance of $D_2^+(X\,\Sigma_g)$ at a time of probing.

the 8 fs pulse is ~5% within a 100 fs window.

We produce three laser pulses with independent delays from one laser pulse, as follows. Because the pulses are so short, we cannot employ conventional beam splitters. We pass the laser beam coaxially through three 1.17-mm-thick fused silica plates. The central 5 mm portion of the beam is the control pulse, the 8 mm ring outside this is the pump pulse, and the remaining outer part of the beam is the probe pulse. Because of their different beam diameters, the probe pulse is most tightly focused and the pump pulse is most loosely focused, so that the probe pulse ionizes a small volume inside the other two foci. Both the probe and control pulses are delayed by rotating the corresponding plate to accumulate an extra optical path. We use a different thickness probe plate (1.46 mm) for a measurement near 500 fs.

To gain experimental control over the intensity, we use a broadband $\lambda/4$ wave plate to elliptically polarize the pulse that passes through the delay plates. All three pulses then reflect off a Brewster-angled germanium plate. This polarizes the pump and probe pulses perpendicular to the TOF axis, thus to the molecular axis. We maintain the elliptical polarization of the control pulse by coating the center of the germanium with gold. The parallel component of the control pulse modifies the $D_2^+(X\,\Sigma_g)$ and $D_2^+(A\,\Sigma_u)$ and gates the dissociation, while the pump and probe pulse do not affect potentials. We adjust the ellipticity so that the parallel component of the control pulse is sufficient to influence the potential. The pump and probe intensity is adjusted, if necessary, by covering part of the beam.

The observed kinetic energy spectrum of D^+ at a probe delay of 34 fs and a control delay of 17 fs is shown as a small figure within Fig. 1. The pump and probe laser intensity is $\sim 1\times 10^{14}$ W/cm^2 and $>5\times 10^{14}$ W/cm^2, respectively. Three peaks are observed, at <2 eV, ~4 eV, and ~11 eV. The <2 eV peak is observed as a background with

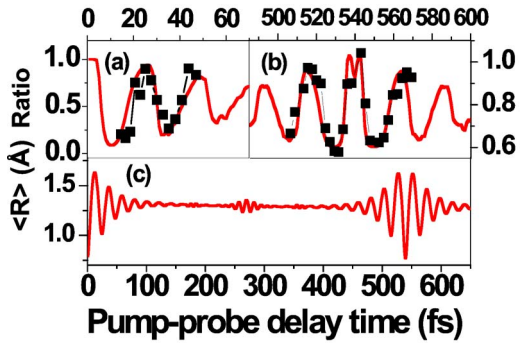

FIG. 2. (Color online) The observed motion of the bound vibrational wave packet (squares right axis) at two different time ranges (a) and (b), without a control pulse. Solid lines in (a) and (b) are the results of a quantum mechanical calculation (left axis; see text). In (c), the calculated expectation value of the vibrational wave function is plotted as a function of pump-probe delay. The vibrational wave packet dephases quickly, but it revives again around ~500 fs.

any of the three pulses. This is due to the low-intensity prepulse before the main 8 fs pulse [12,13]. In the presence of both the pump and probe pulse, the 11 eV peak is observed. If we add the control pulse at 17 fs, then another peak appears at ~4 eV. We adjusted the intensity of the control pulse so that the ~4 eV peak of D^+ in Fig. 1 is only detected when we add the control pulse to the other two pulses ($\sim 1\times 10^{14}$ W/cm^2). Using the D_2^{2+} potential we convert the kinetic energy to internuclear separation. The 11 eV peak corresponds to $R=1.3$ Å, and the 4 eV to 3.6 Å. The peak at ~4 eV is not due to enhanced ionization [14] because the probe laser is polarized perpendicular to the molecular axis.

First, we focus on the bound wave packet motion without the control pulse. As the probe pulse is delayed, the peak in the D^+ spectrum moves between 8 eV and 14 eV corresponding to an internuclear separation of 1.8–1 Å. To follow the motion quantitatively, we calculate the ratio of the signal counts in the range of 6–20 eV to those in the high-energy part (12–20 eV) at a given probe delay. The ratio is plotted as a function of the pump-probe delay as squares in Figs. 2(a) and 2(b) (right axis). We cannot probe at less than 12 fs because the pulses begin to overlap.

The solid lines in Figs. 2(a) and 2(b) are the calculated ratios (left axis) of $\int_0^{1.2\ \text{Å}}|X(R)|^2dR/\int_0^{\infty}|X(R)|^2dR$ as a function of time, where 0–1.2 Å corresponds to the high-energy part and $X(R)$ represents the vibrational wave function obtained by a quantum mechanical calculation. We scale the calculated ratio to fit the experimental data because the structure of the wave packet obtained from a Coulomb explosion can be slightly distorted by the R dependence of the ionization rate from D_2^+ to D_2^{2+}. The agreement between experimental data points and the calculated line shows that the change in kinetic energy distribution reflects the motion of the vibrational wave packet. In Fig. 2(c), we also plot the calculated expectation value $\langle R\rangle$ of the position of the D_2^+ wave packet as a reference.

The calculation shows that the amplitude of the data point's oscillation decreases as the delay increases up to

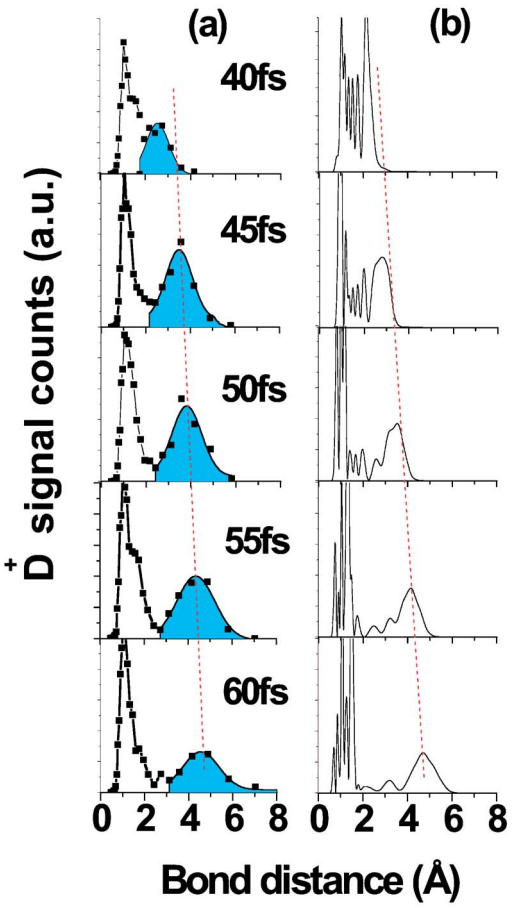

FIG. 3. (Color online) (a) The time evolution of the vibrational wave packet of D_2^+ when the control pulse is applied at 34 fs. The shadowed region propagates to larger internuclear separation with increasing probe time. (b) shows the corresponding calculated wave packet motion.

70 fs due to the wave packet dephasing from the anharmonicity of the $D_2^+(X\,\Sigma_g)$ potential. However, near a delay time of 500 fs, the amplitude revives as Fig. 2(b) shows. The experimental data points follow the calculated line. This corresponds to the first half revival of the vibrational wave packet [15]. The observation of the revival structure can be used to explore the changes of the bound wave packet motion.

Now we turn our attention to controlling the wave packet motion. We apply the control laser pulse to guide part of the vibrational wave packet into the dissociation continuum. Figure 3(a) plots the measured wave packet as a function of the probe delay time at a fixed control time (34 fs), ~1.5 vibrational periods. In the figures, the kinetic energy of the fragment has been converted to internuclear separation using the D_2^{2+} potential as a reference. The contribution from the background has been subtracted from the spectrum.

After the control pulse is applied, the wave packet spreads over the range 1–4 Å and then splits into two. Part of the wave packet remains in the range <2.5 Å and oscillates in the bound potential but because of the dephasing, the motion becomes indistinct. The intensity of the control pulse was sufficiently low that it did not affect the motion of the bound

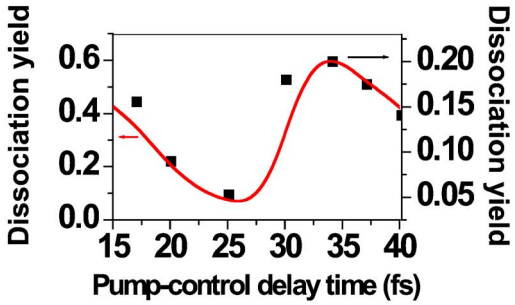

FIG. 4. (Color online) The observed (squares; right axis) relative dissociation yield as a function of the control delay together with the calculated results (solid line; left axis). We scale the data point to fit the calculated curve. The probe time is fixed at 50 fs where the bound and continuum wave packets are well separated.

wave packet: with a higher intensity ($>2\times10^{14}$ W/cm^2) it is possible to control the kinetic energy of the bound wave function by up to 0.3 eV [10]. The other part of the vibrational wave packet continues to dissociate.

We evaluate the average speed of the dissociating wave packet from Fig. 3(a). We fit the data points (2.9–10 Å) by a Gaussian curve, convert kinetic energy (KE) to R, and take the peak as the average position at each probe time. Plotting the average position as a function of probe time, and fitting the data points by a linear curve, we obtain a mean speed of 0.1 ± 0.01 Å/fs (~0.52 eV). The speed depends slightly on the control delay time.

The experimental results can be compared with the square of the calculated vibrational wave function with a control pulse intensity of 1×10^{14} W/cm^2 and a delay of 34 fs, shown in Fig. 3(b). For the calculation we solve the time-dependent Schrödinger equation using a two-state model [10,16,17]. Since the carrier-envelope phase was not fixed in our experiment, we average over different carrier-envelope phases. The calculated average speed of the dissociating wave packet is ~0.12 Å/fs, in agreement with the experiment.

The branching ratio between the bound and continuum wave packet can be controlled by changing the control delay. We fix the probe time at 50 fs where the bound and continuum wave packets are fully separated. We measure the D^+ kinetic energy distribution as a function of the control pulse time from 17 to 40 fs. We integrate the signal counts over 2.4–6 eV, and plot the value as a function of the control delay in Fig. 4 (squares). The solid line is from the calculation. Dissociation is almost entirely suppressed at a control delay of ~25 fs, which corresponds to one vibrational period of D_2^+. This is because if the control pulse is applied when the vibrational wave packet reaches the inner turning point, then the effect of the dipole force is minimized [4].

In conclusion, by combining wave packet motion and laser induced dipole forces applied with subvibrational period precision, we have shown that it is possible to control wave packet dissociation. In more complex molecules, the wave packets will be less well-defined, but the underlying physics will remain valid.

With subvibrational control established, further control is

possible. First, it is technically feasible to apply the control pulse at the 1/4 revival where the wave packet is localized at both turning points. A weak control pulse adds different phases to the outer and inner wave packets. This can qualitatively change subsequent wave packet rephasing and can be used for quantum logic operations [18]. Second, if the carrier-envelope phase of the control laser pulse is controlled, then we can control electron motion while the wave packet dissociates. More than a decade ago it was predicted that an intense phase-controlled pulse could induce a dipole in a strongly driven two level system and hold it fixed while the pulse is present [19]. The D_2^+ wave packet at longer bond distances prepared by our step-by-step approach can produce an ideal two-level system. If the phase-fixed control pulse is applied as the wave packet is near the outer turning point, then the electron is localized on one of the two D^+ ions during the rapid rise of the laser intensity and held fixed while the molecule dissociates. This breaks the left-right symmetry of the dissociation process.

We confirm this mechanism by a quantum mechanical calculation using the two-state model. As long as the laser intensity does not lead to ionization, the electronic and vibrational motion of D_2^+ is well described by using the $D_2^+(X\,\Sigma_g)$ and $D_2^+(A\,\Sigma_u)$ states [17]. We calculate the dissociation asymmetry ($\int_{3\ \text{Å}}^{\infty}|X_R(R)|^2dR/\int_{3\ \text{Å}}^{\infty}|X_L(R)|^2dR$) at the end of the propagation, where $X_R(R)$ and $X_L(R)$ is the dissociating wave packet going right and left. At the control delay of 12 fs, the pulse duration of 8 fs and 1×10^{14} W/cm^2, the dissociation asymmetry changes from 1.88 to 0.53 by π phase changes. It depends on laser intensity, the carrier-envelop phase, and control delay. The probability of finding the ion on one side or the other should be easily observed in a TOF mass spectrometer.

[1] S. A. Rice, Nature (London) **403**, 496 (2001); L. C. Zhu *et al.*, Science **270**, 77 (1995).
[2] R. J. Levis, G. M. Menkir, and H. Rabitz, Science **292**, 709 (2001); T. Brixner, N. H. Damrauer, P. Nikalus, and G. Gerber, Nature (London) **414**, 57 (2001); B. J. Pearson, J. L. White, T. C. Weinacht, and P. H. Bucksbaum, Phys. Rev. A **63**, 063412 (2001).
[3] A. Baltuska *et al.*, Nature (London) **421**, 611 (2003).
[4] H. Niikura, P. B. Corkum, and D. M. Villeneuve, Phys. Rev. Lett. **90**, 203601 (2003).
[5] J. Weiner, V. S. Bagnato, S. Zilio, and P. S. Julienne, Rev. Mod. Phys. **71**, 1 (1999); S. Kuhr *et al.*, Science **293**, 278 (2001).
[6] B. Freidrich and D. Herschbach, Phys. Rev. Lett. **74**, 4623 (1995); H. Stapelfeldt and T. Seideman, Rev. Mod. Phys. **75**, 543 (2003).
[7] H. Sakai, S. Minemoto, H. Nanjo, H. Tanji, and T. Suzuki, Phys. Rev. Lett. **90**, 083001 (2003).
[8] H. Stapelfeldt, H. Sakai, E. Constant, and P. B. Corkum, Phys. Rev. Lett. **79**, 2787 (1997).
[9] H. Niikura *et al.*, Nature (London) **417**, 917 (2002).
[10] H. Niikura, D. M. Villeneuve, and P. B. Corkum, Phys. Rev. Lett. **92**, 133002 (2004).
[11] G. Steinmeyer *et al.*, Science **286**, 1507 (1999).
[12] F. Légaré *et al.*, Phys. Rev. Lett. **91**, 093002 (2003).
[13] A. Zavriyev, P. H. Bucksbaum, J. Squier, and F. Salin, Phys. Rev. Lett. **70**, 1077 (1993).
[14] T. Seideman, M. Yu. Ivanov, and P. B. Corkum, Phys. Rev. Lett. **75**, 2819 (1995).
[15] I. S. Averbukh and N. F. Perelman, Phys. Lett. A **139**, 449 (1989).
[16] F. Châteauneuf *et al.*, J. Chem. Phys. **108**, 3974 (1998).
[17] I. Kawata, H. Kono, and Y. Fujimura, J. Chem. Phys. **110**, 11152 (1999).
[18] K. Lee, D. M. Villeneuve, P. B. Corkum, and E. A. Shapiro, Phys. Rev. Lett. **93**, 233601 (2004).
[19] M. Y. Ivanov, P. B. Corkum, and P. Dietrich, Laser Phys. **3**, 375 (1993).